

34. Falkowski, P. G. & Raven, J. A. *Aquatic Photosynthesis* (Blackwell Science, Malden, 1997).
 35. Woods, J. D., Barkmann, W. & Strass, V. in *The Ocean Surface* (eds Toba, Y. & Mitsuyasu, H.) 487–507 (Reidel, Dordrecht, 1985).

Acknowledgements

We thank all scientists, officers and crew aboard the RRS *Discovery* for assistance, P. Liss and T. Jinkells for leadership during fieldwork, W. Broadgate for setting up the cruise, P. Machine and G. Monocoiffé of the BODC for CTD and accessory data management, J. Grimalt for analytical facilities, and R. Kiene and K. Ledyard for providing accessory information to published data. R. Kiene also provided valuable comments. This work was supported by the Spanish CICYT through the Programa Nacional de Ciencia y Tecnología Marinas (CyTMAR) and the British NERC through the Atmospheric Chemistry Studies in the Oceanic Environment (ACSOE) Community Programme.

Correspondence and requests for materials should be addressed to R.S. (e-mail: rsimo@icm.csic.es).

The effect of climate change on ozone depletion through changes in stratospheric water vapour

Daniel B. Kirk-Davidoff, Eric J. Hints, James G. Anderson & David W. Keith

Department of Earth and Planetary Sciences and Department of Chemistry and Chemical Biology, Harvard University, Cambridge, Massachusetts 02138, USA

Several studies have predicted substantial increases in Arctic ozone depletion due to the stratospheric cooling induced by increasing atmospheric CO₂ concentrations^{1,2}. But climate change may additionally influence Arctic ozone depletion through changes in the water vapour cycle. Here we investigate this possibility by combining predictions of tropical tropopause temperatures from a general circulation model with results from a one-dimensional radiative convective model, recent progress in understanding the stratospheric water vapour budget, modelling of heterogeneous reaction rates and the results of a general circulation model on the radiative effect of increased water vapour³. Whereas most of the stratosphere will cool as greenhouse-gas concentrations increase, the tropical tropopause may become warmer, resulting in an increase of the mean saturation mixing ratio of water vapour and hence an increased transport of water vapour from the troposphere to the stratosphere. Stratospheric water vapour concentration in the polar regions determines both the critical temperature below which heterogeneous reactions on cold aerosols become important (the mechanism driving enhanced ozone depletion) and the temperature of the Arctic vortex itself. Our results indicate that ozone loss in the later winter and spring Arctic vortex depends critically on water vapour variations which are forced by sea surface temperature changes in the tropics. This potentially important effect has not been taken into account in previous scenarios of Arctic ozone loss under climate change conditions.

The winter/spring depletion of ozone in the polar vortex is determined by (1) halogen activation, (2) sunlight (which drives the photochemical reactions that catalytically destroy ozone) and (3) deactivation of chlorine to reservoir species. Because of the dependence on insolation, ozone is most sensitive to active chlorine in the spring. Halogens are activated—converted to free-radical form—in nearly every Arctic winter, when temperatures fall below about 195 K. Deactivation occurs at different times each year, depending on stratospheric temperatures and dynamics. For example, the 1996–97 winter had particularly severe ozone depletion because the Arctic vortex stayed cold later, even though

temperatures were not particularly low⁴. Increases in the concentration of water vapour in the atmosphere raise the threshold temperature for halogen activation, thus allowing polar processing to continue later in the season and maintaining high concentrations of ClO. In a warm winter with temperatures near the threshold for chlorine activation, increases in water vapour may allow activation to occur when it would otherwise not. Thus, ozone losses will not simply scale with chlorine loading in the stratosphere in coming decades.

Previous studies of the relationship between climate change and ozone depletion have focused on the influence of increasing carbon dioxide on polar stratospheric temperatures, and thus on heterogeneous ozone chemistry^{1,2}. Recent progress in the observation and understanding of the stratospheric water vapour budget^{5,6} now makes possible an evaluation of the chain linking greenhouse-gas increases to warming in the tropics, increased water vapour in the stratosphere, increased aerosol activity in the polar vortices, and thus increased high-latitude ozone depletion. Because ozone depletion depends so strongly on the presence of temperatures low enough to initiate heterogeneous chemistry, we adopt $(T_\alpha - T_v)$ as a predictor of ozone loss, where T_v is the temperature of the polar vortex, and T_α is the temperature below which heterogeneous chemistry on aerosols becomes important, yielding dramatic increases in the concentration of ClO. We can express the rest of this chain mathematically as follows:

$$\frac{\partial(T_\alpha - T_v)}{\partial T_s} = \frac{\partial(T_\alpha - T_v)}{\partial [H_2O]_v} \frac{\partial [H_2O]_v}{\partial [H_2O]_e} \frac{\partial [H_2O]_e}{\partial T_e} \frac{\partial T_e}{\partial T_s} \quad (1)$$

T_e is the temperature of the tropical tropopause, T_s is the surface temperature in the tropics, $[H_2O]_e$ is the concentration of water vapour entering the tropical stratosphere, and $[H_2O]_v$ is the concentration of water vapour in the polar vortices. We treat here only those variations in T_e due to changes in the tropical climate (and reflected in changes in T_s), thus neglecting changes in T_e due, for instance, to changes in stratospheric circulation. We have also neglected the terms $\partial T_e / \partial p_e$ and $\partial [H_2O]_e / \partial p_e$, where p_e is the pressure at which air enters the stratosphere (that is, the pressure of the tropical tropopause), because, as we will discuss, we believe $\partial p_e / \partial T_s$, the dependence of tropical tropopause pressure on tropical surface temperature, to be small.

We begin by considering $\partial(T_\alpha - T_v) / \partial [H_2O]_v$. To evaluate this term we must analyse the dependence of ozone depletion on temperature and water vapour. To a good approximation, the time rate of change of ozone in the polar vortices is given by the sum of the rate-limiting steps of catalytic cycles involving ClO and

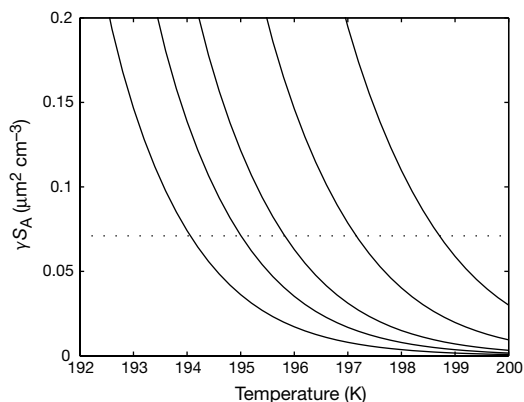


Figure 1 Temperature and water dependence of γS_A at 50 mbar. S_A is the aerosol surface area, and γ is the reaction probability per collision for the reaction $HCl + ClONO_2$. Curves are plotted for water vapour concentrations of 5, 6, 7, 9 and 12 p.p.m.v., from left to right. $\partial T_\alpha / \partial [H_2O]_v$ is evaluated along the dotted line, which indicates the value of γS_A at the temperature (195 K) at which heterogeneous ozone depletion is observed to become significant for the present water vapour mixing ratio of ~6 p.p.m.v.

BrO (ref. 7).

$$\frac{d[\text{O}_3]}{dt} = -2k_{\text{ClO}-\text{ClO}}[\text{ClO}]^2 - 2k_{\text{ClO}-\text{BrO}}[\text{ClO}][\text{BrO}] \quad (2)$$

The total ozone loss is the integral of this loss rate over the volume of the region where ClO is elevated. In the Arctic vortex, unlike the Antarctic, destruction of ozone is never complete, so that both the loss rate and the volume and duration of the region in which ozone loss occurs are important⁸.

The concentration of ClO depends on the partitioning of total inorganic chlorine between ClO and the reservoir species HCl and ClONO₂. In the polar vortices, this partitioning is controlled by heterogeneous reactions of the reservoir species on surfaces, yielding ClO. The quadratic dependence on [ClO] means that the ozone loss rate is very sensitive to increases of both $\gamma_{\text{HCl}+\text{ClONO}_2}$, the reaction rate of gaseous ClONO₂ with HCl on aerosols, and S_A , the aerosol surface area per unit volume, as temperature decreases or water vapour increases⁹. Denitrification is also important, and is expected to enhance ozone depletion in a future atmosphere with lower chlorine loading and lower temperatures (and increased water vapour) by limiting deactivation of ClO to ClONO₂ (ref. 10).

Figure 1 shows curves of γS_A plotted versus T_v for various values of $[\text{H}_2\text{O}]_v$. As $[\text{H}_2\text{O}]_v$ increases, so does the temperature (T_α) at which γS_A rises abruptly. The temperature–water vapour dependence of S_A is taken from ref. 11, and that of γ from ref. 12. These relationships have been substantially verified by aircraft measurements of ClO (ref. 13).

Using the data presented in Fig. 1, we can evaluate $\partial T_\alpha/\partial[\text{H}_2\text{O}]_v$ for a range of water vapour mixing ratios. We note that in the present conditions, $[\text{H}_2\text{O}]_v$ is ~ 6 p.p.m.v. (ref. 14), and that heterogeneous ozone depletion chemistry becomes important at temperatures below 195 K (at 50 mbar). We thus choose $\gamma S_A = 0.071$ as the value of γS_A corresponding to T_α . We can then set $\partial T_\alpha/\partial[\text{H}_2\text{O}]_v = \partial T/\partial[\text{H}_2\text{O}]$ evaluated along the parametric curve $\gamma S_A(T, [\text{H}_2\text{O}]) = c$, where $c = 0.071$. For present conditions, $\partial T_\alpha/\partial[\text{H}_2\text{O}]_v = 0.8$ K p.p.m.v.⁻¹. This value is insensitive to variation in c , but decreases logarithmically with increasing $[\text{H}_2\text{O}]_v$, falling to 0.7 K p.p.m.v.⁻¹ for $[\text{H}_2\text{O}]_v = 8$ p.p.m.v.

Forster and Shine have recently evaluated $\partial T_v/\partial[\text{H}_2\text{O}]_v$ (ref. 3). Using both a general circulation model (GCM) and a column model, they found that a uniform increase of 0.7 p.p.m.v. of water vapour in the stratosphere resulted in a cooling of the polar vortices by 4–6 K in the spring, implying that $\partial T_v/\partial[\text{H}_2\text{O}]_v$ ranges from 6 to 9 K p.p.m.v.⁻¹. Thus, the radiative effect of an increase in water vapour on vortex temperature dwarfs the chemical effect of such an increase discussed above. They point out, however, that the net cooling effect of observed changes in stratospheric CO₂, H₂O and O₃ over-predicts the observed stratospheric temperature trends by a factor of 2 or more. Thus, either the stratospheric water vapour trend or stratospheric climate modelling has large errors.

We next consider $\partial[\text{H}_2\text{O}]_v/\partial[\text{H}_2\text{O}]_e$. Air reaches the polar vortices along trajectories high in the stratosphere, without mixing with air below the 380 K potential temperature surface¹⁵. Thus water vapour concentrations in the polar vortices are governed predominantly by the concentration of water vapour and CH₄ entering the stratosphere in the tropics, and $\partial[\text{H}_2\text{O}]_v/\partial[\text{H}_2\text{O}]_e$ is therefore ~ 1.0 . Oxidation of CH₄ adds about 2 p.p.m.v. of water vapour to air in the polar vortices¹⁴ but has an insignificant effect on $\partial[\text{H}_2\text{O}]_v/\partial[\text{H}_2\text{O}]_e$.

Recent improvements in our understanding of the tropical tropopause indicate that $\partial[\text{H}_2\text{O}]_e/\partial T_e$ can be evaluated to useful accuracy simply by assuming that $[\text{H}_2\text{O}]_e = [\text{H}_2\text{O}]^*(T_e, p_e)$, where $[\text{H}_2\text{O}]^*(T, p)$ is the saturation mixing ratio of water vapour as a function of temperature and pressure. T_e and p_e are the temperature and pressure at the tropopause, defined as the altitude of minimum temperature, and the bar represents an average over all tropopause points in the range 10° S to 10° N. A careful examination of radiosonde temperature measurements along with a survey of relevant

stratospheric water vapour and CH₄ measurements⁵ has shown that $[\text{H}_2\text{O}]^*(T_e, p_e)$, calculated from radiosonde data, is consistent with observations of stratospheric water vapour. Furthermore, a Green's function analysis of water vapour and CO₂ profiles shows that seasonal variations of tropical stratospheric water vapour are consistent with variations in the mean of daily tropopause saturation mixing ratios in sounding data¹⁶. This assumption allows us to calculate $\partial[\text{H}_2\text{O}]_e/\partial T_e$ using the Clausius–Clapeyron equation. Present tropopause mean temperature and pressure of 191 K and 95 mbar imply a value of 0.8 p.p.m.v. K⁻¹. $\partial[\text{H}_2\text{O}]_e/\partial T_e$ itself increases with temperature, rising to 1.0 p.p.m.v. K⁻¹ at 193 K, and 1.4 p.p.m.v. K⁻¹ at 195 K, assuming p_e remains constant.

To estimate the value of $\partial T_e/\partial T_s$, we turn to modelling studies of the structure of the atmosphere's response to increased greenhouse-gas loading. We first consider output of the National Center for Atmospheric Research (NCAR) CCM3 atmospheric model¹⁷ coupled with a slab ocean model, and run to equilibrium at pre-industrial and at doubled CO₂ concentrations (J. T. Kiehl, personal communication). The temperature difference between the two equilibria (Fig. 2) increases from the surface upwards through the upper troposphere, since the convection parametrization tends to adjust the tropical atmosphere towards a moist-adiabatic lapse rate. In the region of the tropopause, the temperature difference abruptly shifts from large positive values to large negative values, yielding a change of 1.0 K in T_e for a change of 1.5 K in T_s . However, the model's low resolution means that it cannot predict changes in tropopause height which might accompany a warming of the tropics.

To evaluate the possible changes in the height of the tropopause, we investigated the behaviour of a one-dimensional radiative–convective model^{18,19} with enhanced resolution (2.5 mbar) in the neighbourhood of the tropopause, and a cooling term of 0.5 K d⁻¹ added in the stratosphere and upper troposphere to represent the Brewer–Dobson circulation. In this model, the height of the tropopause remains constant under a wide variety of climate-change scenarios, lending support to the use of the GCM to predict tropopause temperature changes. However, the temperature change at the tropopause in this model is generally larger than in GCMs for the same change in surface temperature: 2.4 K for a 1.5 K warming at the surface. Here we use the NCAR CCM3 prediction as the conservative basis for our estimate of the change in tropical tropopause temperature and saturation water vapour pressure, and thus of the change in polar vortex water vapour in a

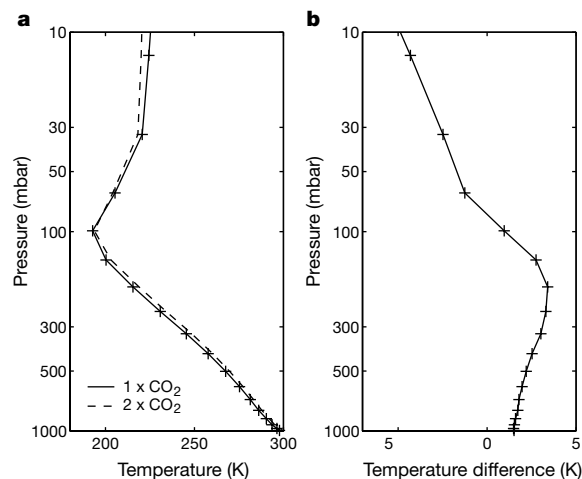


Figure 2 GCM simulation of tropical vertical temperature profile. **a**, Tropical mean (10° S–10° N) temperatures from NCAR CCM3 atmospheric model coupled with a slab ocean, and run to equilibrium with pre-industrial (1 × CO₂, solid line) and doubled (2 × CO₂, dashed line) carbon dioxide concentrations. **b**, Tropical mean temperature difference (2 × CO₂ – 1 × CO₂).

Table 1 Terms relating ozone depletion to greenhouse forcing

Derivative	Estimated value	References
$\frac{\partial T_v}{\partial [H_2O]_v}$	-6 to -9 K p.p.m.v. ⁻¹	3
$\frac{\partial T_\alpha}{\partial [H_2O]_v}$	0.8 K p.p.m.v. ⁻¹	
$\frac{\partial [H_2O]_v}{\partial [H_2O]_b}$	1.0	25, 13
$\frac{\partial [H_2O]_b}{\partial T_o}$	0.8 p.p.m.v. K ⁻¹	5
$\frac{\partial T_o}{\partial T_s}$	0.7 (GCMs)–1.6 (1-D model)	
dT_s	1–4 K (W ⁻¹ m ²)	20

doubled-CO₂ climate. Another GCM, the Goddard Institute for Space Studies (GISS) atmospheric model²⁰, predicts a similar ratio of tropopause warming to surface warming, with equilibrium tropical tropopause warming of 2.0 K for 3.1 K at the surface in a run with doubled CO₂ (R. Ruedy, personal communication). Thus, we estimate $\partial T_o/\partial T_s$ to be 0.7. Use of the high-resolution one-dimensional radiative convective model would yield an estimate of 1.6.

We now estimate the effect of climate change on ozone depletion via water vapour changes. Table 1 lists estimated values and references for each of the derivatives in equation (1). Multiplying these out, and assuming a relatively small value for $\partial T_v/\partial [H_2O]_v$ of -6 K p.p.m.v.⁻¹ we obtain $\partial(T_\alpha - T_v)/\partial T_s = 3.8$. Thus, since GCM estimates of equilibrium tropical surface warming range from 1 to 4 K (ref. 21), this yields an increase in $(T_\alpha - T_v)$ of 3.8–11.4 K (accepting the one-dimensional model results would roughly double these numbers). This increase is large when compared with model predictions^{22,23} of the direct cooling effect in the Arctic vortex of doubling CO₂, which range from 2 K to 3.5 K. Shindell *et al.* showed that a 5 K cooling of the Arctic vortex led to a springtime destruction of ~50% of ozone within the Arctic vortex in the decade 2010–19, compared to ~15% depletion at present¹. Our results increase our confidence that at least this much cooling will occur.

Measurements of CH₄ concentration, and calculations of CH₄ sources and sinks, suggest that CH₄ concentrations may not grow much above current levels²⁴. If CH₄ concentrations were to resume growth at the rate observed during the 1980s, increasing CH₄ flux to the stratosphere might be expected to contribute another 1.3 p.p.p.v. of water vapour to the polar vortex mixing ratio by the year 2100. This would yield an additional increase of ~0.9 K in T_α .

Several studies have attempted to calculate trends based on observations of stratospheric water vapour. *In situ* frost-point hygrometer measurements yield a trend of 0.01–0.03 p.p.m.v. yr⁻¹ for the years 1981–94 (ref. 25). Observations using a photofragment fluorescence hygrometer aboard the NASA ER-2 show no significant trend in stratospheric water vapour over the years 1993–97 (ref. 6), while observations from space show trends in water vapour mixing ratio of 0.04–0.10 p.p.m.v. yr⁻¹ for the years 1991–96 (ref. 26). Since the last two trends are based on relatively short time series, they may have little to do with longterm climate variations. A trend of 0.04 p.p.m.v. yr⁻¹ is equivalent to a tropopause temperature trend of 0.05 K yr⁻¹ at the tropopause, so any connection between observed trends in stratospheric water vapour and trends in tropospheric climate will be difficult to detect, given the sparseness of tropical radiosonde measurements.

There are several sources of uncertainty in our calculations. The first is our continuing ignorance of the exact mechanism by which water vapour enters the stratosphere. If the cold-point tropopause temperature is actually controlled by convecting parcels reaching

that level, conservation of entropy by those parcels might lead to even larger increases in the cold-point tropopause temperature as surface temperature rises. Our results provide a strong motivation for the improvement of our understanding and observation of the tropical tropopause region and its sensitivity to changes in radiative and convective forcing. The second is the wide range of predicted changes in tropical surface temperature as greenhouse-gas concentrations increase. Last, a change in the stratospheric overturning circulation may affect polar chemistry in several ways: by changing the tropical tropopause temperature^{27,28}, by changing the temperature of persistence of the polar vortex¹, or by changing the average age of vortex air and thus the amount of water added by methane oxidation. All these effects need to be considered in assessing the effect of altered stratospheric dynamics. □

Received 15 March; accepted 18 October 1999.

- Shindell, D. T., Rind, D. & Loneragan, P. Increased polar stratospheric ozone losses and delayed eventual recovery owing to increasing greenhouse-gas concentrations. *Nature* **392**, 589–592 (1998).
- Austin, J., Butchart, N. & Shine, K. P. Possibility of an Arctic ozone hole in a doubled-CO₂ climate. *Nature* **360**, 221–225 (1992).
- Forster, P. M. & Shine, K. P. Stratospheric water vapour changes as a possible contributor to observed stratospheric cooling. *Geophys. Res. Lett.* (in the press).
- Chipperfield, M. P. & Pyle, J. A. Model sensitivity studies of Arctic ozone depletion. *J. Geophys. Res.* **103**, 28389–28403 (1998).
- Dessler, A. E. A reexamination of the “stratospheric fountain” hypothesis. *Geophys. Res. Lett.* **25**, 4165–4168 (1998).
- Hurst, D. F. *et al.* Closure of the total hydrogen budget of the northern extratropical lower stratosphere. *J. Geophys. Res.* **104**, 8191–8200 (1999).
- Anderson, J. G., Toohey, D. W. & Brune, W. H. Free-radicals within the Antarctic vortex—the role of CFCs in Antarctic ozone loss. *Science* **251**, 39–46 (1991).
- Müller, R. *et al.* Severe chemical ozone loss in the Arctic during the winter of 1995–96. *Nature* **389**, 709–712 (1997).
- Hofmann, D. J. & Oltmans, S. J. The effect of stratospheric water vapor on the heterogeneous reaction rate of ClONO₂ and H₂O for sulfuric acid aerosol. *Geophys. Res. Lett.* **19**, 2211–2214 (1992).
- Waibel, A. E. *et al.* Arctic ozone loss due to denitrification. *Science* **283**, 2064–2069 (1999).
- Carlsaw, K. S., Luo, B. & Peter, T. An analytic expression for the composition of aqueous HNO₃-H₂SO₄ stratospheric aerosols including gas phase removal of HNO₃. *Geophys. Res. Lett.* **22**, 1877–1880 (1995).
- Hanson, D. R. & Ravishankara, A. R. Reactive uptake of ClONO₂ onto sulfuric acid due to reaction with HCl and H₂O. *J. Phys. Chem.* **98**, 5728–5735 (1994).
- Kawa, S. R. *et al.* Activation of chlorine in sulfate aerosol as inferred from aircraft observations. *J. Geophys. Res.* **102**, 3921–3933 (1997).
- Schiller, C. *et al.* The partitioning of hydrogen species in the Arctic winter stratosphere: Implications for microphysical parameters. *J. Geophys. Res.* **101**, 14489–14493 (1996).
- Holton, J. R. *et al.* Stratosphere-troposphere exchange. *Rev. Geophys.* **33**, 403–439 (1995).
- Andrews, A. E. *et al.* Empirical age spectra for the lower tropical stratosphere from *in situ* observations of CO₂: Implications for stratospheric transport. *J. Geophys. Res.* (in the press).
- Hack, J. J., Kiehl, J. T. & Hurrell, J. W. The hydrologic and thermodynamic characteristics of the NCAR CCM3. *J. Clim.* **11**, 1179–1206 (1998).
- Emanuel, K. A. A scheme for representing cumulus convection in large-scale models. *J. Atmos. Sci.* **48**, 2313–2335 (1991).
- Chou, M. D. & Suarez, M. J. *An Efficient Thermal Radiation Parameterization for Use in General Circulation Models* (NASA Tech. Memorandum 104606, Vol.3, NASA Goddard Space Flight Center, Greenbelt, Maryland, 1994).
- Hansen, J. *et al.* Forcing and chaos in interannual to decadal climate change. *J. Geophys. Res.* **102**, 25679–25720 (1997).
- Kattenberg, A. *et al.* in *Climate Change 1995* (eds Houghton, J. T. *et al.*) 285–358 (Cambridge Univ. Press, 1996).
- Rind, D., Suozzo, R., Balachandran, N. K. & Prather, M. J. Climate change and the middle atmosphere. Part I: The doubled CO₂ climate. *J. Atmos. Sci.* **47**, 475–494 (1990).
- Colman, R. A., Power, S. B., McAvaney, B. J. & Dahn, R. R. A non-flux corrected transient CO₂ experiment using the BMRC coupled atmosphere/ocean GCM. *Geophys. Res. Lett.* **22**, 3047–3050 (1995).
- Dlugokencky, E. J. *et al.* Continuing decline in the growth rate of the atmospheric CH₄ burden. *Nature* **393**, 447–450 (1998).
- Oltmans, S. J. & Hofmann, D. J. Increase in lower-stratospheric water vapour at a mid-latitude Northern Hemisphere site from 1981 to 1994. *Nature* **374**, 146–149 (1995).
- Nedoluha, G. E. *et al.* Increases in middle atmospheric water vapor as observed by the Halogen Occultation Experiment and the ground-based Water Vapor Millimeter-wave Spectrometer from 1991 to 1997. *J. Geophys. Res.* **103**, 3531–3543 (1998).
- Reid, G. C. & Gage, K. S. The tropical tropopause over the western Pacific: wave driving, convection, and the annual cycle. *J. Geophys. Res.* **101**, 21233–21241 (1996).
- Fells, S. B. Radiative-dynamical interactions in the middle atmosphere. *Adv. Geophys.* **A 28**, 277–300 (1985).

Acknowledgements

We thank J. Kiehl for sharing output from the NCAR CCM3 GCM. This work was supported by NASA.

Correspondence and requests for materials should be addressed to D.B.K.-D. (e-mail: davidoff@huarp.harvard.edu). The updated model code from ref. 18 is available at <http://texmex.mit.edu/pub/emanuel/CONRAD>.